Electronic Supplementary Material (ESI) for Nanoscale.

Supporting information

Selenium-Enriched Hollow $NiCo_2O_4$/NiO Heterostructured Nanocages as Efficient Electrocatalyst for Oxygen Evolution Reaction

Vaibhav Namdev Kale, T. Maiyalagan*

Electrochemical Energy Laboratory, Department of Chemistry, SRM Institute of Science and Technology, Kattankulathur, Tamilnadu, India.

*E-mail address- maiyalagan@gmail.com & maiyalat@srmist.edu.in

EXPERIMENTAL SECTION

Material Characterizations

In this study, the morphological features, nanostructures and elemental analysis were analyzed by scanning electron microscope (SEM, Thermoscientific Apreo S) and high-resolution transmission electron microscope (HR-TEM) and TEM (HRTEM, JEOL Japan, JEM-2100 Plus instrument)) including the energy dispersive spectrometer (EDS) mapping analysis. The synthesized materials underwent powder X-ray diffraction (XRD) (X'pert pro diffractometer, PANalytical) for the microstructural analysis and were further subjected to XPS analysis utilizing system: the Shimadzu ESCA 3400 instrument (Physical Electronics system; monochromatic beam 1486.6 eV) with an AlKα source operated at 15 kV, for identification of the elements spectra that confirms of the elements existed in the prepared sample and used to study surface properties.

Electrochemical Measurements

All electrochemical measurements were conducted by using a potentiostat (AUTOLAB, PGSTAT204). To run all the electrochemical experiments the three-electrode setup was employed and the setup consisted of Hg/HgO electrode, platinum wire and glassy carbon (GC) electrode used as a reference, counter and the working electrode, respectively, under N_2 saturated 1.0 M KOH electrolyte. LSV (Linear sweep voltammetry) measurements were performed at the operated potential window of 1.02–1.82 V (vs. RHE) and achieved at a scan rate of 5 mV/s. The EIS (electrochemical impedance spectroscopy) analysis was used for the investigation of the OER process kinetics in the frequency range of 100 kHz–0.1 Hz. The Nova 2.1 software was used for electrochemical impedance data fitting. All the voltages were converted to vs. RHE according to the following Eq. $E_{(RHE)} = E_{(Hg/HgO)} + 0.059\ pH + E^0$, where $E^0 = 0.098$ V) [S1]. A

chronoamperometry test was conducted to inspect the electrochemical stability towards OER at a fixed voltage of 1.52 V vs. RHE.

CALCULATION METHODS

Calculation of ECSA

The following equation is used to calculate the electrochemically active surface area (ECSA), which is proportional to the electrochemical double-layer capacitance (C_{dl}). The equation is as follows:

$$ECSA = \frac{C_{dl}}{C_s} [S2]$$

Where C_s is a constant specific electrochemical capacitance of 0.04 mF cm ^{2}. By plotting the graph of capacitive current density which was measured using cyclic voltammetry (CV) as a function of scan rate, the C_{dl} values of the catalyst were determined from the slope of linear fitted curves [S1].

Calculation of Roughness Factor (RF)

The electrochemical double-layer capacitance (C_{dl}) measurements are used to calculate the roughness factor (RF) of the as-synthesized catalysts using the following equation:

$$RF = \frac{ECSA}{Geometric\ area\ of\ the\ electrode} [S3]$$

Mass activity

The mass activities of the electrocatalysts were calculated by dividing the delivered current density (j) with the catalyst mass loading (m = 0.245 mg cm^{-2}) at an overpotential (η) of 320 mV.

$$Mass\ activity = \frac{j}{m} \quad [S4]$$

(a)

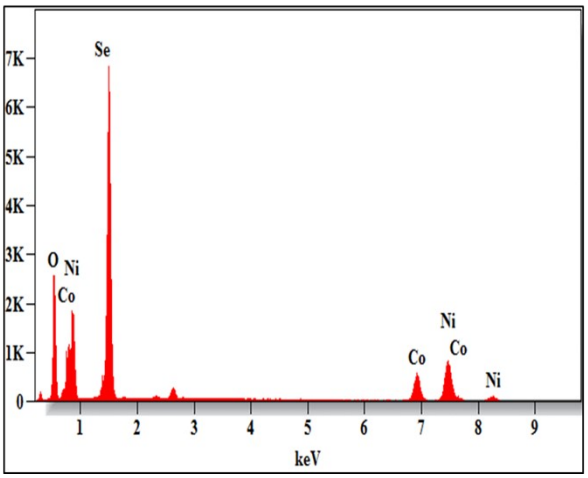

(b)

Element	Weight %	Atom %
Ni	39.73	21.43
Co	22.05	11.84
O	32.60	64.48
Se	5.62	2.25
Total	100.00	100.00

Figure S1. (a, b) Energy dispersive spectroscopy (EDS) spectrum and elemental composition of 5 wt% Se-$NiCo_2O_4$/NiO.

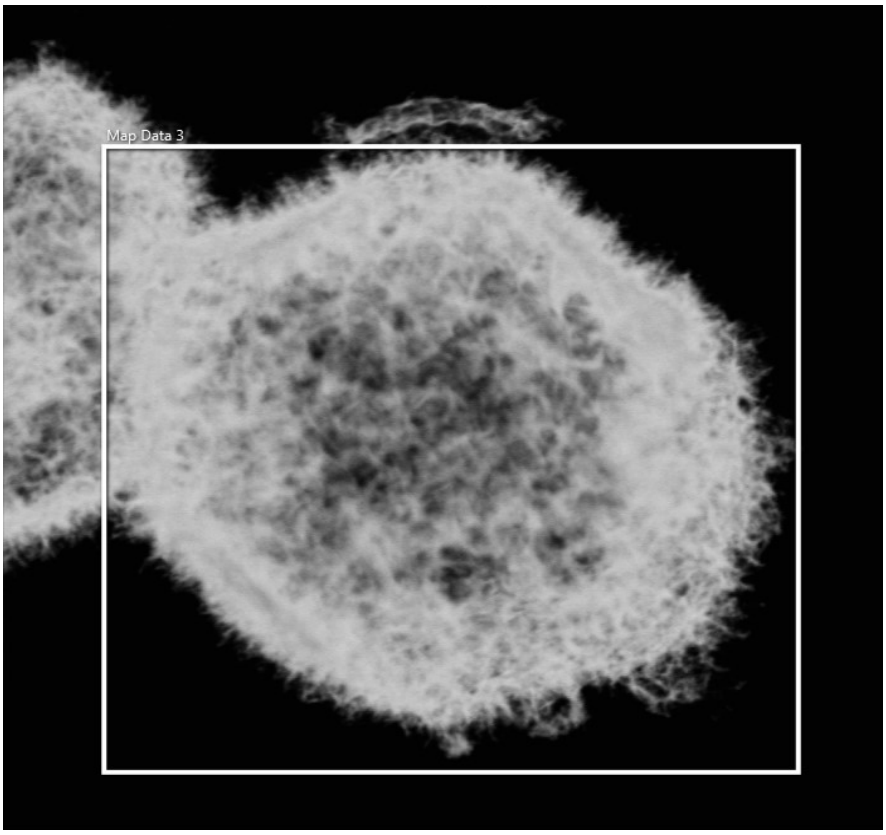

Figure S2. TEM mapping image of 5 wt% Se-$NiCo_2O_4$/NiO.

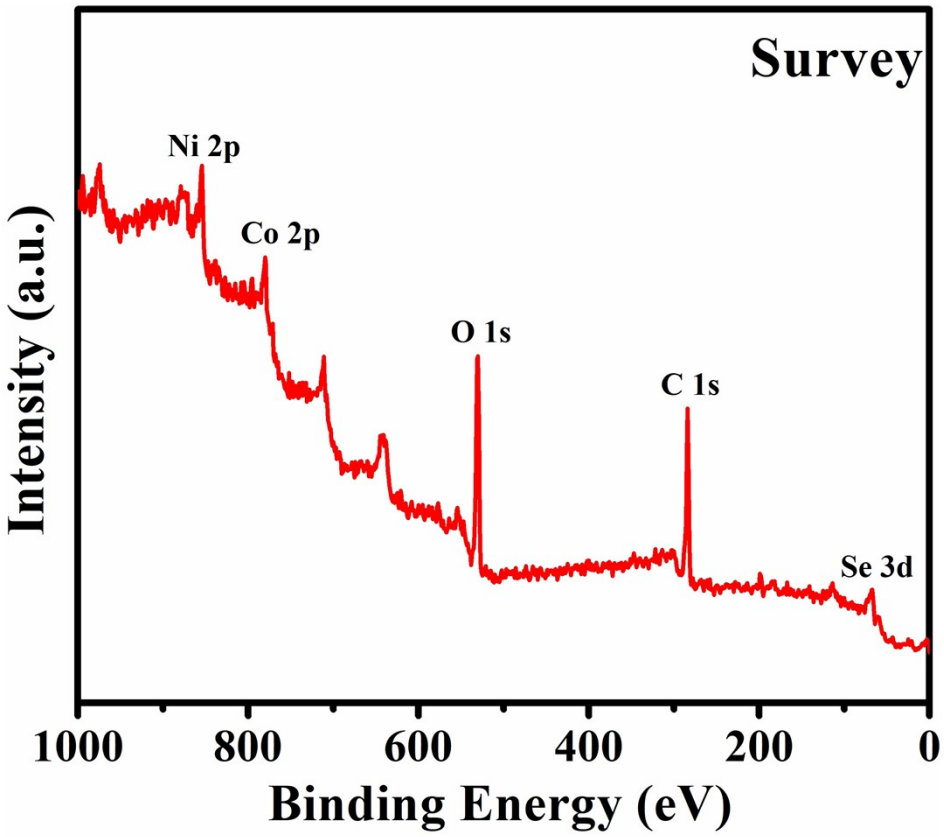

Figure S3. XPS survey spectrum of 5 wt% Se-$NiCo_2O_4$/NiO.

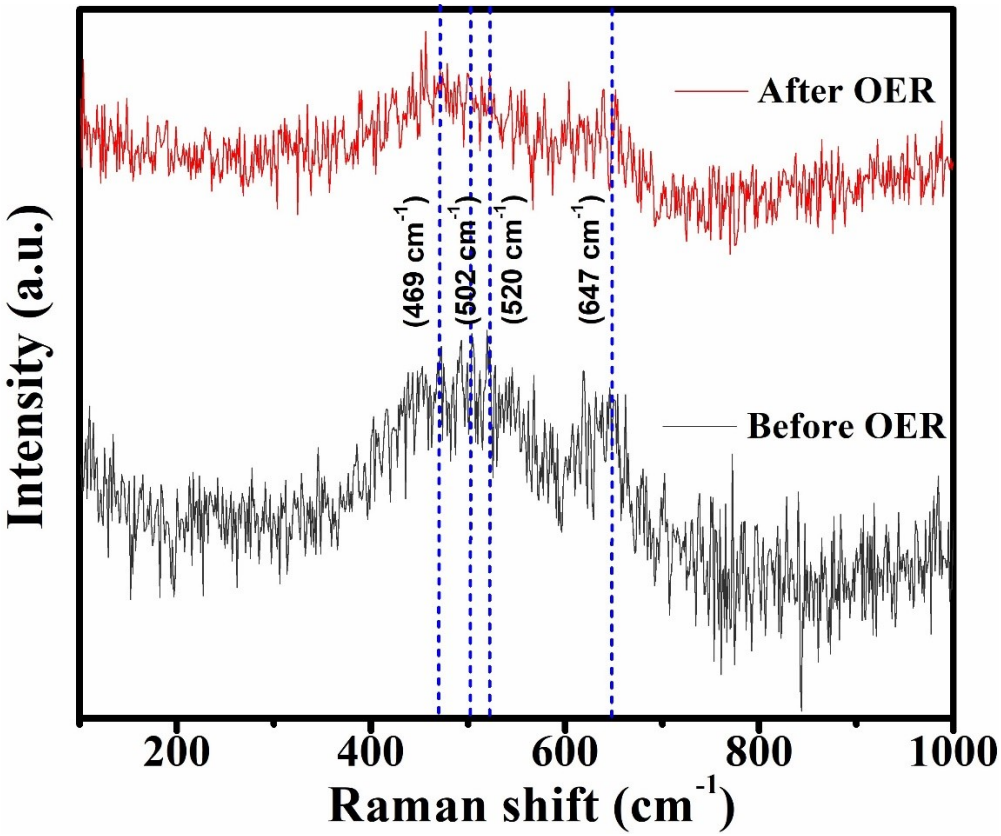

Figure S4. Raman analysis of 5 wt% Se-$NiCo_2O_4$/NiO before and after electrochemical stability.

(a)

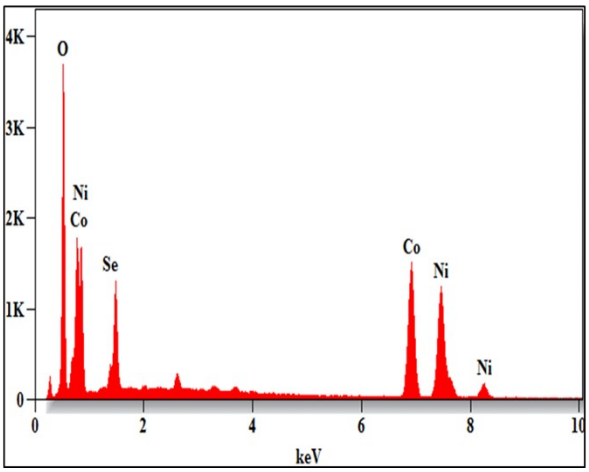

(b)

Element	Weight %	Atom %
Ni	34.60	20.27
Co	20.42	10.68
O	41.83	67.68
Se	3.15	1.37
Total	100.00	100.00

Figure S5. (a, b) Energy dispersive spectroscopy (EDS) spectrum and elemental composition of 5 wt% Se-$NiCo_2O_4$/NiO after OER stability test.

Table S1. Various parameters were obtained from the deconvoluted XPS spectrum of 5 wt% Se-$NiCo_2O_4$/NiO.

Element	Peak	B.E. (eV)	FWHM
Ni 2p	Ni^{2+} ($2p_{3/2}$)	854.4	1.53
	Ni^{2+} ($2p_{1/2}$)	872.8	3.30
	Sat.	861.8	4.85
	Ni^{3+} ($2p_{3/2}$)	856.2	2.89
	Ni^{3+} ($2p_{1/2}$)	876.1	3.80
	Sat.	880.6	4.0
Co 2p	Co^{3+} ($2p_{3/2}$)	780.2	2.47
	Co^{3+} ($2p_{1/2}$)	795.2	2.59
	Sat.	787.3	4.90
	Co^{2+} ($2p_{3/2}$)	782.4	3.85
	Co^{2+} ($2p_{1/2}$)	797.6	3.69
	Sat.	803.4	4.70
O 1s	O1	530.1	1.49
	O2	531.5	1.85
	O3	532.6	2.42
Se 3d	$3d_{5/2}$	53.7	2.45
	$3d_{3/2}$	55.9	1.95
	Se – O	60.6	3.46

B.E= Binding Energy FWHM= Full Width Half Maxima

Table S2. Comparison of the electrochemical OER activity of the as-prepared NiCo-LDH, 5 wt% Se-NiCo-LDH, 10 wt% Se-NiCo-LDH, $NiCo_2O_4$/NiO, 5 wt% Se- $NiCo_2O_4$/NiO and 10 wt% Se-$NiCo_2O_4$/NiO electrocatalysts.

Catalyst	E_{onset} **(V)**	η_{onset} **(mV)**	E_{OER} **(V) at 10 mA cm ^{2}**	η **(mV) at 10 mA cm ^{2}**	j **at 1.82 V (mA cm ^{2})**
NiCo-LDH	1.489	259	1.569	338	56.41
5 wt% Se-NiCo-LDH	1.454	224	1.536	306	68.11
10 wt% Se-NiCo-LDH	1.465	235	1.541	311	63.19
$NiCo_2O_4$/NiO	1.475	245	1.553	323	71.48
5 wt% Se-$NiCo_2O_4$/NiO	1.440	210	1.518	288	86.32
10 wt% Se-$NiCo_2O_4$/NiO	1.452	222	1.531	301	73.46

E_{onset} = Onset potential E_{OER} = OER potential j = Current density

η_{onset} = Onset overpotential η = Overpotential

Table S3. Corresponding values of the Tafel Slope, Solution Resistance and Charge-Transfer Resistance of of the as-prepared NiCo-LDH, 5 wt% Se-NiCo-LDH, 10 wt% Se-NiCo-LDH, $NiCo_2O_4$/NiO, 5 wt% Se- $NiCo_2O_4$/NiO and 10 wt% Se- $NiCo_2O_4$/NiO electrocatalysts.

Catalyst	**Tafel slope mV dec ^{1}**	R_s **(Ω)**	R_{ct} **(Ω)**
NiCo-LDH	117.5	7.21	15.4
5 wt% Se-NiCo-LDH	107.9	6.31	10.6
10 wt% Se-NiCo-LDH	116	7.07	11.6
$NiCo_2O_4$/NiO	76.4	6.24	14.2
5 wt% Se-$NiCo_2O_4$/NiO	66.7	6.12	7.65
10 wt% Se-$NiCo_2O_4$/NiO	87.3	5.83	9.51

R_s =Solution resistance R_{ct}= Charge transfer resistance

Table S4. Electrochemical performance of the as-prepared NiCo-LDH, 5 wt% Se-NiCo-LDH, 10 wt% Se-NiCo-LDH, $NiCo_2O_4$/NiO, 5 wt% Se- $NiCo_2O_4$/NiO and 10 wt% Se- $NiCo_2O_4$/NiO electrocatalysts.

Catalyst	C_{dl} **(mF cm ^{2})**	**ECSA (cm^2)**	**Mass Activity (A g^{-1}) @1.55 V vs. RHE**	R_F
NiCo-LDH	0.183	4.57	28.02	23.31
5 wt% Se-NiCo-LDH	0.344	8.6	53.28	43.87
10 wt% Se-NiCo-LDH	0.336	8.4	48.24	42.85
$NiCo_2O_4$/NiO	0.354	8.85	28.57	45.1
5 wt% Se-$NiCo_2O_4$/NiO	1.7	42.5	90.36	216.8
10 wt% Se-$NiCo_2O_4$/NiO	0.587	14.6	64.32	74.4

Table S5. Comparison of the OER performance of some previously reported electrocatalysts in an alkaline electrolyte with the 5 wt% Se-$NiCo_2O_4$/NiO electrocatalysts developed in this study.

Electrocatalyst	**Electrolyte**	**Substrate**	**η_{10} (mV)**	**Tafel slope mV dec ^{1}**	**References**
Se-$NiCo_2O_4$/NiO (MOF-derived)	**1 M KOH**	**GCE**	**288**	**66.7**	**This work**
NiO/$NiCo_2O_4$-rGO (MOF-derived)	1 M KOH	GCE	340	66	S5
NiO/$NiCo_2O_4$ Nanofibers	1 M KOH	GCE	357	130	S6
$NiCoO_2$@CeO_2 Nanoboxes	1 M KOH	GCE	380	72	S7
$NiCo_2O_4$/NiO Nanosheets	1 M NaOH	GCE	360	61	S8
$NiCo_2O_4$/NiO@N/S-C (MOF-derived)	1 M KOH	GCE	285	53	S9
Co_3O_4/$NiCo_2O_4$/NF (MOF-derived)	0.1 M KOH	NF	320	84	S10
Co_3O_4/$NiCo_2O_4$ DSNCs (MOF-derived)	1 M KOH	NF	340	88	S11
CFP/$NiCo_2O_4$/$Co_{0.57}Ni_{0.43}$LMOs	0.1 M KOH	CFP	340	63	S12
NiO/CoN PINWS	1 M KOH	CFP	300	35	S13
$NiCo_2O_4$@$NiCo_2O_4$ Microspheres	1 M KOH	GCE	350	70	S14
U-NiO/$NiCo_2O_4$	0.1 M KOH	GCE	387	49	S15

GCE= Glassy carbon electrode CFP= carbon fiber paper NF= Nickel foam

Table S6. The elemental composition of the hollowed 5 wt% Se-NiCo2O4/NiO nanocages before and after stability testing through EDS.

Element	Before stability		After stability	
	Weight %	**Atom %**	**Weight %**	**Atom %**
Ni	39.73	21.43	34.60	20.27
Co	22.05	11.84	20.42	10.68
O	32.60	64.48	41.83	67.68
Se	5.62	2.25	3.15	1.37

References

S1. J. Yan, L. Kong, Y. Ji, J. White, Y. Li, J. Zhang, P. An, S. Liu, S. T. Lee and T. Ma, Single atom tungsten doped ultrathin α-$Ni(OH)_2$ for enhanced electrocatalytic water oxidation, *Nat. Commun.*, 2019, **10**, 2149.

S2. Y. Chen, H. Wu, N. Tang, Y. Zhang and Y. Wang, $NiCo_2S_4$ octahedral configuration doped by Mn, Zn and Cu for oxygen evolution reaction, *ChemComm*, 2024.

S3. S. Shit, S. Chhetri, W. Jang, N. C. Murmu, H. Koo, P. Samanta, T. Kuila, Cobalt sulfide/nickel sulfide heterostructure directly grown on nickel foam: an efficient and durable electrocatalyst for overall water splitting application, *ACS Appl. Mater. Interface*, 2018, **10**, 27712-27722.

S4. J. Zhou, Z. Han, X. Wang, H. Gai, Z. Chen, T. Guo, X. Hou, L. Xu, X. Hu, M. Huang and S. V. Levchenko, Discovery of quantitative electronic structure-OER activity relationship in metal-organic framework electrocatalysts using an integrated theoretical-experimental approach, *Adv. Funct. Mater*., 2021, **31**, 2102066.

S5. Y. Wang, Z. Zhang, X. Liu, F. Ding, P. Zou, X. Wang, Q. Zhao and H. Rao, MOF-derived NiO/$NiCo_2O_4$ and NiO/$NiCo_2O_4$-rGO as highly efficient and stable electrocatalysts for oxygen evolution reaction, *ACS Sustain. Chem. Eng.*, 2018, **6**, 12511-12521.

S6. Z. Zhang, X. Liang, J. Li, J. Qian, Y. Liu, S. Yang, Y. Wang, D. Gao and D. Xue, Interfacial engineering of NiO/$NiCo_2O_4$ porous nanofibers as efficient bifunctional catalysts for rechargeable zinc–air batteries, *ACS Appl. Mater. Interfaces*, 2020, **12**, 21661-21669.

S7. L. Cao, J. Cai, W. Deng, , Y. Tan and Q. Xie, $NiCoO_2$@CeO_2 nanoboxes for ultrasensitive electrochemical immunosensing based on the oxygen evolution reaction in a neutral

medium: Application for interleukin-6 detection, *Anal. Chem.*, 2020, **92**, 16267-16273.

S8. C. Mahala and M. Basu, Nanosheets of $NiCo_2O_4$/NiO as efficient and stable electrocatalyst for oxygen evolution reaction, *ACS Omega*, 2017, **2**, 7559-7567.

S9. Y. Yuan, L. Sun, Y. Li, W. Zhan, X. Wang and X. Han, Synergistic modulation of active sites and charge transport: N/S Co-doped C encapsulated $NiCo_2O_4$/NiO hollow microrods for boosting oxygen evolution catalysis, *Inorg. Chem.*, 2020, **59**, 4080-4089.

S10. M. Yang, W. Lu, R. Jin, X. C. Liu, S. Song and Y. Xing, Superior oxygen evolution reaction performance of Co_3O_4/$NiCo_2O_4$/Ni foam composite with hierarchical structure*, ACS Sustain. Chem. Eng.*, 2019, **7**, 12214-12221.

S11. H. Hu, B. Guan, B. Xia and X. W. Lou, Designed formation of Co_3O_4/$NiCo_2O_4$ double-shelled nanocages with enhanced pseudocapacitive and electrocatalytic properties, *J. Am. Chem. Soc.*, 2015, **137**, 5590-5595.

S12. J. Yin, P. Zhou, L. An, L. Huang, C. Shao, J. Wang, H. Liu and P. Xi, Self-supported nanoporous $NiCo_2O_4$ nanowires with cobalt–nickel layered oxide nanosheets for overall water splitting, *Nanoscale*, 2016, **8**, 1390-1400.

S13. J. Yin, Y. Li, F. Lv, Q. Fan, Y. Q. Zhao, Q. Zhang, W. Wang, F. Cheng, P. Xi and S. Guo, NiO/CoN porous nanowires as efficient bifunctional catalysts for Zn–air batteries, *ACS Nano*, 2017, **11**, 2275-2283.

S14. J. Zhao, F. W. Chen, X. Y. Zhao, X. J. Wang, Y. P. Li and F. T. Li, Self-Composition of Hierarchical Core–Shell-Structured $NiCo_2O_4$@$NiCo_2O_4$ Microspheres with Oxygen Vacancies for Efficient Oxygen Evolution Electrocatalysis, *Energy Fuels*, 2023, **37**, 18111–18119.

S15. A. Cetin and E. N. Esenturk, Hierarchical nanowire and nanoplate-assembled $NiCo_2O_4$–NiO biphasic microspheres as effective electrocatalysts for oxygen evolution reaction, *Mater. Today Chem.*, 2019, **14**, 100215.